

Stereospecific Polymerization of Propylene with Group 4 *ansa*-Fluorenylamidodimethyl Complexes

Kei Nishii^a, Hideaki Hagihara^b, Tomiki Ikeda^a, Munetaka Akita^a and Takeshi Shiono^{c,*}

^a *Chemical Resources Laboratory, Tokyo Institute of Technology,*

Nagatsuta-cho 4259, Midori-ku, Yokohama 226-8503, Japan

^b *National Institute of Advanced Industrial Science and Technology (AIST)*

Polymer Synthesis Team Macromolecular Technology Research Center

Central 5, 1-1 Higashi, Tsukuba, 305-8565 Japan

^c *Department of Applied Chemistry, Graduate School of Engineering,*

Hiroshima University, Higashi-Hiroshima 739-8527, Japan.

*Corresponding author: Fax: +81 82 424 5494. E-mail: tshiono@hiroshima-u.ac.jp

ABSTRACT

Group 4 $[\eta^1:\eta^3\text{-}tert\text{-butyl}(\text{dimethylfluorenylsilyl})\text{amido}]\text{dimethyl complexes } [t\text{-BuNSiMe}_2\text{Flu}]\text{MMe}_2$ (M = Ti, **1**; Zr, **2**; Hf, **3**) were synthesized in a one-pot synthesis starting from the ligand, MeLi and MCl₄ (M = Ti, Zr, Hf), respectively. The structures of these complexes were determined by X-ray crystallography and the results obtained revealed that the fluorenyl ligand coordinates to center metal in a η^3 -manner irrespective of center metal employed. Propylene polymerization was conducted at 0 or 20 °C in toluene by **1–3** combined with dried methylaluminumoxane (MAO), which was prepared from the toluene solutions of MAO by removing free trialkylaluminiums, and HNMe₂PhB(C₆F₅)₄ in the presence of triisobutylaluminium. The **1**-dried MAO system gave the polymer with syndiotactic triad (rr) of 63% at 0 °C, whereas **2** and **3** did not

give any polymer in the same conditions. The **2**-dried MAO system gave the polymer with the highest syndiotacticity ($rr = 97\%$) at $20\text{ }^{\circ}\text{C}$, although the activity was low. The **3**-dried MAO system did not give any polymer even at $20\text{ }^{\circ}\text{C}$. When $\text{HNMe}_2\text{PhB}(\text{C}_6\text{F}_5)_4$ was used in place of dried MAO at $20\text{ }^{\circ}\text{C}$, **1** gave almost atactic polymer, while **2** and **3** gave highly syndiotactic one ($rr \approx 90\%$). These results indicate that the catalytic performance strongly depended on the center metal of the *ansa*-fluorenylamidodimethyl complexes as well as cocatalysts employed.

Keywords: syndiotactic, atactic, metallocene catalysts, polypropylene

1. Introduction

Since the discovery of metallocene catalysts, a great number of organometallic compounds have been applied for olefin polymerization as so-called single-site catalysts from both the academic and the industrial points of view [1]. During the first half of the 1990's, Bercaw [2], Okuda [3], the researchers of Dow [4] and Exxon [5] reported a new type of half metallocene complexes which contain the N-based ligand attached to the cyclopentadiene derivatives, named *ansa*-monocyclopentadienylamido (CpA) complex [1c, 6]. The CpA complexes have been found to be highly efficient catalysts for synthesis of linear low-density polyethylene and copolymerization of ethylene and styrene [4, 5, 7]. Several researchers reported the synthesis of a series of group 4 CpA complexes and the influence of the ligand in CpA complexes on the stereospecificity and the regiospecificity of propylene polymerization [8]. Okuda et al. prepared *tert*-butylamidofluorenylzirconium complexes for potentially syndiospecific catalyst [9]. We have found that $[\textit{t}\text{-BuNSiMe}_2\text{Flu}]\text{TiMe}_2$ (**1**) activated with methylaluminoxane (MAO), $\text{B}(\text{C}_6\text{F}_5)_3$ or $\text{Ph}_3\text{CB}(\text{C}_6\text{F}_5)_4$ promoted the polymerization of propylene at $40\text{ }^{\circ}\text{C}$ in syndiospecific and highly regiospecific manner [10]. Razavi et al. and Busico et al.

reported the introduction of *tert*-butyl group on the fluorenyl ligand ($[t\text{-BuNSiMe}_2(2,7\text{-di-}t\text{-Bu-Flu})]\text{TiCl}_2$, $[t\text{-BuNSiMe}_2(3,6\text{-di-}t\text{-Bu-Flu})]\text{TiCl}_2$) increased the syndiospecificity and activity [11].

Shiomura et al. reported that the activation of $[t\text{-BuNSiMe}_2\text{Flu}]\text{ZrCl}_2$ with MAO- $i\text{-Bu}_3\text{Al}$ gave syndiotactic polypropylene (PP) ($[\text{rrrr}] = 77\%$), whereas the activation with $\text{Ph}_3\text{CB}(\text{C}_6\text{F}_5)_4\text{-}i\text{Bu}_3\text{Al}$ gave isotactic PP ($[\text{mmmm}] = 95\%$) [12]. Recently, Fujita et al. reported that the nature of the center metal had a significant effect on catalytic performance and the microstructures of produced PPs using group 4 bis(phenoxy-imine) complex-based catalysts [13]. These results indicate that stereoregularity of PPs obtained should be controlled by the kinds of counter anion and the kinds of center metal.

We have previously reported that **1** activated with $\text{B}(\text{C}_6\text{F}_5)_3$ produced syndiotactic-enriched PP at $-50\text{ }^\circ\text{C}$ in a living manner [14a] and the replacement of $\text{B}(\text{C}_6\text{F}_5)_3$ with trialkylaluminum (Me_3Al , $i\text{Bu}_3\text{Al}$)-free MAO, named dried MAO and dried modified MAO (MMAO), raised the living polymerization temperature up to $0\text{ }^\circ\text{C}$ accompanied by the improvement of syndiospecificity [14b, c]. These results suggest that stereospecificity and propylene polymerization behavior in the complex **1**-based catalysts strongly depend on the cocatalyst and polymerization conditions employed.

In this paper, we synthesized a series of group 4 *ansa*-fluorenylamidodimethyl complexes by applying the synthetic method reported by Resconi et al. [15] and investigated the effects of center metal and cocatalyst on the catalytic performance of propylene polymerization.

2. Experimental part

2.1. Materials

Dimethylaniliniumtetrakis(pentafluorophenyl)borate ($\text{HNMe}_2\text{PhB}(\text{C}_6\text{F}_5)_4$) and

toluene solution of MAO were donated from Tosoh-Finechem Co. Ltd. Dried MAO was prepared from the toluene solution of MAO by vacuum drying followed by washing with hexane as reported previously [14b]. Research grade propylene (Takachiho Chemicals Co.) was purified by passing it through columns of NaOH, P₂O₅, and molecular sieves 3A, followed by bubbling it through a NaAlH₂Et₂/1,2,3,4-tetrahydronaphthalene solution. All solvents were commercially obtained and dried with standard methods.

2.2. Synthesis of *t*-BuNSiMe₂Flu (Flu = C₁₃H₉) Ligand

All the syntheses were carried out under N₂ by standard Schlenk techniques. The *t*-BuNHSiMe₂Flu ligand was prepared according to the literature (Scheme 1) [9, 16]. To a solution of fluorene (24 g, 144 mmol) in diethyl ether (300 mL) was added *n*-butyllithium (96 mL, 1.50 M solution in hexane, 144 mmol) at 0 °C within 1 h. After stirring for 3 h at room temperature, the solvent was removed in vacuo to give Li[Flu]. To a solution of excess dichlorodimethylsilane (40 mL) was added the suspension of Li[Flu] in hexane (250 mL) at -78 °C. The resultant suspension was stirred for 8 h at room temperature, and the solvent and the remained dichlorodimethylsilane were removed in vacuo. Lithium chloride was precipitated and the solution was decanted, followed by removal of the solvent, 34.2 g (132 mmol) of 9-(chlorodimethylsilyl)fluorene was obtained as off-white solid.

To a solution of 9-(chlorodimethylsilyl)fluorene 34.2 g (132 mmol) in THF (200 mL) was added *t*-butylamine (20 mL, 264 mmol) at 0 °C. Stirring overnight at room temperature gave a yellow-orange suspension. Lithium chloride was precipitated and the solution was decanted. Removal of the solvent gave *t*-BuNHSiMe₂Flu as yellow oil (28.5 g, 96.5 mmol, 67% yield). ¹H NMR (C₆D₆, ref. C₆H₆: 7.15 ppm): 7.79 (d, 2H,

C₁₃H₉), 7.61 (d, 2H, C₁₃H₉), 7.29 (dd, 4H, C₁₃H₉), 3.76 (s, 1H, C₁₃H₉), 1.02 (s, 9H, C(CH₃)₃), 0.42 (s, 1H, NH), -0.09 (s, 6H, Si(CH₃)₂).

2.3. Synthesis of [*t*-BuNSiMe₂Flu]TiMe₂ (**1**)

To a solution of *t*-BuNHSiMe₂Flu (1.56 g, 5.28 mmol) in Et₂O (50 mL) was slowly added excess MeLi (24.0 mL of a 1.20 M solution in Et₂O, 28.2 mmol) at room temperature and the mixture was stirred for 5 h. To TiCl₄ (0.58 mL, 5.29 mmol) diluted with 50 mL of pentane was added a solution of the dilithium salt in Et₂O at room temperature. The resulting dark brown suspension was stirred overnight at room temperature. After the solvent was removed, the residue was extracted with hexane (120 mL) and the hexane solution was decanted. To the hexane solution was added MeMgBr (3.0 mL of a 3.0 M solution in ether), and the resulting mixture was stirred for 5 h at room temperature. After the solvent was removed, the residue was extracted with hexane (80 mL). The hexane solution was concentrated and cooled overnight at -30 °C to give **1** (route **I** in Scheme 1) as yellow-orange microcrystals (0.840 g, 2.26 mmol, 42.8%). ¹H NMR (C₆D₆): δ = -0.02 (s, 6H, TiCH₃), 0.67 (s, 6H, SiCH₃), 1.37 (s, 9H, C(CH₃)₃), 7.09 (ddd, 2H, C₁₃H₈) 7.22 (ddd, 2H, C₁₃H₈), 7.67 (dd, 2H, C₁₃H₈), 7.82 (dd, 2H, C₁₃H₈). ¹³C NMR (C₆D₆): δ = 135.0, 129.2, 127.8, 127.7, 124.8, 123.7 (C₁₃H₈), 58.6 (C(CH₃)₃), 56.7 (Ti(CH₃)₂), 34.3 (C(CH₃)₃), 5.7 (Si(CH₃)₂). Anal. Calcd for C₂₁H₂₉NSiTi: C, 67.91; H, 7.87; N, 3.77. Found: C, 68.03; H, 7.87; N, 3.89.

2.4. Synthesis of [*t*-BuNSiMe₂Flu]ZrMe₂ (**2**)

The same procedure for the preparation of **1** was applied except ZrCl₄ was used in the final step. The hexane solution was concentrated and cooled overnight at -30 °C to give **2** as yellow microcrystals (yield, 42.4%). ¹H NMR (C₆D₆): δ = -0.58 (s, 6H, ZrCH₃),

0.74 (s, 6H, SiCH₃), 1.29 (s, 9H, C(CH₃)₃), 7.13–7.16 (m, 4H, C₁₃H₈) 7.77–7.80 (m, 4H, C₁₃H₈).). ¹³C NMR (C₆D₆): δ = 136.2, 128.7, 125.7, 124.2, 123.8 (C₁₃H₈), 55.6 (C(CH₃)₃), 41.4 (Zr(CH₃)₂), 34.9 (C(CH₃)₃), 7.0 (Si(CH₃)₂). EI-MS: *m/z* = 413 (M⁺).

2.5. Synthesis of [*t*-BuNSiMe₂Flu]HfMe₂ (**3**)

The same procedure for the preparation of **1** was applied except HfCl₄ was used in the final step. The hexane solution was concentrated and cooled overnight at –30 °C to give **3** as light-yellow needle crystals (yield, 42.2%). ¹H NMR (C₆D₆): δ = –0.80 (s, 6H, HfCH₃), 0.77 (s, 6H, SiCH₃), 1.26 (s, 9H, C(CH₃)₃), 7.14–7.16 (m, 4H, C₁₃H₈) 7.78–7.80 (m, 4H, C₁₃H₈).). ¹³C NMR (C₆D₆): δ = 136.6, 128.9, 125.5, 124.1, 123.8 (C₁₃H₈), 72.8 (C⁹ of C₁₃H₈), 54.8 (C(CH₃)₃), 51.4 (Hf(CH₃)₂), 35.3 (C(CH₃)₃), 7.0 (Si(CH₃)₂). EI-MS: *m/z* = 502 (M⁺).

2.6. Polymerization Procedure

Polymerization was performed in a 100-mL glass reactor equipped with a magnetic stirrer as follows. Toluene as solvent was placed in the reactor. After the solvent was saturated with gaseous propylene under atmospheric pressure, polymerization was started by successive addition of prescribed amounts of cocatalyst and catalyst. The propylene pressure and temperature were kept constant during the polymerization. Polymerization was conducted for a prescribed time, and quenched by addition of HCl/methanol solution. The polymers obtained were adequately washed with methanol and dried under vacuum at 60 °C for 6 h.

2.7. Analytical Procedures

Molecular weight and molecular weight distribution of PPs obtained were determined by gel permeation chromatography (GPC) with a Waters 150CV at 140 °C using *o*-dichlorobenzene as a solvent. The parameters for universal calibration were $K = 7.36 \times 10^{-5}$, $\alpha = 0.75$ for polystyrene standard and $K = 1.03 \times 10^{-4}$, $\alpha = 0.78$ for PP sample.

The ^1H NMR spectra of complexes were measured at room temperature on a JEOL GX500 spectrometer operated at 500.00 MHz in pulse Fourier-Transform mode. The pulse angle was 45° and 64 scans were accumulated in pulse repetition of 7.0 s. The ^{13}C NMR spectra of PPs were measured at 120 °C on a JEOL GX 500 spectrometer operated at 125.65 MHz in the pulse Fourier-transform mode. The pulse angle was 45° and about 5,000 scans were accumulated in pulse repetition of 5.0 s. Sample solutions were prepared in 1,1,2,2-tetrachloroethane- d_2 up to 10 wt-%. The central peak of 1,1,2,2-tetrachloroethane (74.47 ppm) was used as an internal reference.

EI-MS (electron impact mass spectrum) was recorded on a JEOL JMS-SX 102A mass spectrometer at 30 eV.

Differential scanning calorimetry (DSC) analysis was performed on a Seiko DSC-220. The samples were encapsulated in aluminum pans and annealed at 80 °C for 4 hours to ensure sufficient time for crystallization. After annealing, the DSC curves of the samples were recorded under a nitrogen atmosphere with a heating rate of 10 °C/min from 20 to 200 °C.

2.8. X-ray Structure Determination

Single crystals were mounted on glass fibers. Diffraction measurements were made on a Rigaku RAXIS IV imaging plate area detector with Mo $K\alpha$ radiation ($\lambda = 0.71069$ Å). Indexing was performed from 2 oscillation images, which were exposed for 5 min. The crystal-to-detector distance was 110 mm. Readout was performed with the pixel

size of 100 μm \times 100 μm . Neutral scattering factors were obtained from the standard source [17]. In the reduction of data, Lorentz and polarization corrections and empirical absorption corrections were made [18].

The structural analysis was performed on an IRIS O2 computer using teXsan structure solving program system obtained from the Rigaku Corp., Tokyo, Japan [19]. In the reduction of data, Lorentz and polarization corrections were made. An empirical absorption correction was also made [20]. The structures were solved by a combination of the direct methods (SHELXS-86) [20] and Fourier synthesis (DIRDIF94) [21]. Least-squares refinements were carried out using SHELXL-97 [20] (refined on F^2) linked to teXsan. All the non-hydrogen atoms were refined anisotropically. The methyl hydrogen atoms except the hydrogen atoms attached to the carbon atoms sitting on a crystallographic mirror plane, were refined using riding models, and the other hydrogen atoms were fixed at the calculated positions.

3. Results and Discussion

3.1. Synthesis and Crystal Structures of Complexes

The synthetic routes of dimethylfluorenylsilylamine ligand and its complexation with group 4 metal are summarized in Scheme 1.

(Scheme 1)

The reaction of $\text{Me}_2\text{Si}(\text{Flu})\text{Cl}$ ($\text{Flu} = \text{C}_{13}\text{H}_8$) with excess *tert*- BuNH_2 [6, 16] in THF at room temperature afforded the ligand, *t*- $\text{BuNSiMe}_2\text{Flu}$, [9] in a high yield, as described in the experimental section.

The route **II** in Scheme 1 is the conventional three-step synthetic procedure for the syntheses of group 4 *ansa*-fluorenylamidodimethyl complexes [5c, 10, 22].

Resconi et al. have recently reported the synthesis of group 4 metallocene dimethyl complexes [15b] and CpA dimethyl complexes [15a] from the ligand, a 2-fold excess of MeLi and MCl₄ (M = Ti, Zr, Hf), in a one-pot synthesis as shown by route **I** in Scheme 1.

We applied this method for the synthesis of group 4 *ansa*-fluorenylamidodimethyl complexes and could isolate [*tert*-butyl(dimethylfluorenylsilyl)amido]dimethyl complexes [*t*-BuNSiMe₂Flu]MMe₂ (M = Ti (**1**), Zr (**2**), Hf (**3**)) as yellow-orange microcrystals of **1**, yellow microcrystals of **2** and light-yellow needle crystals of **3**, respectively.

¹H NMR spectra of **1**, **2** and **3** show that the methyl groups bonded to Si and transition metal atoms are equivalent, respectively. The result suggests that N atom is trigonal planar and all complexes are C_s-symmetric in C₆D₆ solution. The single-crystal X-ray diffraction analysis of **1**, **2**, and **3** were performed, and the structures obtained are displayed in Figures 1, 2 and 3, respectively. Crystallographic data and parameters are listed in Table 1. Selected bond lengths and angles are given in Table 2.

(Figure 1, 2 and 3)

(Table 1 and 2)

The bond lengths: Ti(1)–C(3), –C(4), –C(5), –C(6) and –C(7) of tetramethylcyclopentadienylamidodimethyltitanium complex ([*t*-BuNSiMe₂Cp*]TiMe₂) [23] and heterocycle-fused-indenylsilylamidodimethyltitanium complex ([*t*-BuNSiMe₂(*N*-Et-5,6-dihydroindeno[2,1-*b*]indol-6-yl)]TiMe₂) [15c], in which the Cp* and indenyl group coordinate to the Ti atom with a η⁵-manner, are ranging from 2.283 to 2.463 Å and from 2.271 to 2.557 Å, respectively. The Ti(1)–C(6) and Ti(1)–C(7) lengths of **1** are about 0.110 Å longer than those of the Cp* complex, and 0.015–0.032 Å longer than those of the heterocycle-fused indenyl complex. The results suggest that the Flu ligand in **1** should coordinate to the Ti atom in a η³-manner rather than in a η⁵-

manner. Chart 1 shows various bonding modes of Flu ligands found in ansa and simple metallocens by X-ray diffraction studies [24], which are the mode η^5 bonded to the five-membered ring of the Flu ligand (a), η^3 bonded (b), e.g. in $(\eta^5:\eta^3\text{-CpSiMe}_2\text{Flu})\text{YCl}_2\text{Li}(\text{OEt}_2)_2$ [25] and $(\eta^5:\eta^3\text{-Flu})_2\text{Sm}(\text{THF})_2$ [26], and symmetrically η^1 bonded (c) as in $\text{Me}_2\text{Si}(\eta^1\text{-Flu}')(\eta^1\text{-N-}t\text{-Bu})\text{ZrCl}_2\cdot\text{OEt}_2$ (Flu' = $\text{C}_{29}\text{H}_{36}$) [27].

(Chart 1)

The molecular structure of **2** was similar to that of $[t\text{-BuNSiMe}_2\text{Flu}]\text{Zr}(\text{SiMe}_3)_2$ [9], $[t\text{-BuNSiMe}_2\text{Flu}]\text{ZrCl}_2$ [28] and $[t\text{-BuNSiMe}_2(3,6\text{-di-}t\text{-Bu-Flu})]\text{ZrCl}_2$ [11b], in which the Flu group coordinate to the zirconium atom with a η^5 -manner. Okuda et al. suggested that the Flu ligand was bonded in a fashion between η^5 and η^3 , as judged by Zr ring-carbon distances ranging from 2.400 to 2.708 Å in $[t\text{-BuNSiMe}_2\text{Flu}]\text{Zr}(\text{SiMe}_3)_2$. The bond lengths of Zr(1)–C(6) and –C(7) in **2** are about 0.058 or 0.035 Å longer than those of $[t\text{-BuNSiMe}_2\text{Flu}]\text{ZrCl}_2$ and $[t\text{-BuNSiMe}_2(3,6\text{-}t\text{-Bu}_2\text{-Flu})]\text{ZrCl}_2$. Meunier et al. and Rieger et al. have recently reported that the Flu group coordinates to the Zr atom with a η^3 -manner in $[\text{Me}_2\text{Si}(\text{isodicyclopentadienyl})(\text{Flu})]\text{ZrCl}_2$ [29a] or *rac*-[Et(Flu)(2-MeBenz[*b*]indeno[4,5-*d*]thiophen-1-yl)]ZrCl₂, [29b] in which the Zr–C lengths are ranging from 2.408 to 2.763 Å or from 2.404 to 2.696 Å. Considering the complexes described above, the coordination mode of **2** could be also a η^3 -manner.

As compared **2** with **3**, the Zr(1)–C(1,2) lengths are ca. 0.021 Å longer than the Hf(1)–C(1,2) lengths. Other differences can probably be neglected. The results described above suggested that reduced hapticity (η^3) of the Flu ligand in **1-3** are retained in the single-crystal state.

The bond angles of N(1)–M(1)–C(4) in **1** is larger than those of **2** and **3**. The result suggests that **1** should present the most open space for the catalytic active site among the

three complexes.

3.2. Polymerization of Propylene Activated with Dried MAO

Propylene polymerization was conducted at 0 and 20 °C in toluene by **1–3** combined with dried MAO. The results are summarized in Table 3.

(Table 3)

The complex **1** combined with dried MAO gave PP with the highest activity at 0 °C. We have previously reported that the system conducted syndiospecific polymerization in a living manner [14b]. On the other hand, **2** and **3** did not give any polymer in the same conditions. The ¹³C NMR spectrum of the methyl region of PP obtained is shown in Figure 4a.

(Figure 4)

The triad analysis showed that the produced polymer with **1** was syndiotactic-enriched (rr = 63%) as reported previously [14b].

The polymerization with **2** was, therefore, conducted at 20 °C. Although the activity was low, the produced PP was highly syndiotactic (rr = 97% in Figure 4b) with the melting temperature of 124 °C. In addition, the signals arising from regioerror units were not observed in the NMR spectrum of **2** similarly to that of **1**. Although the complex **2** that possesses the non-substituted Flu ligand activated with dried MAO system showed the low polymerization activity, Miller et al. recently reported that the steric expanded zirconium Flu-amido complex (Me₂Si(η¹-Flu')(η¹-N-*t*-Bu)ZrCl₂•OEt₂, Flu' = C₂₉H₃₆)-MAO system showed high activity for propylene polymerization and gave the highly syndiotactic polymer with the highest melting point reported so far [27].

The *N* value in entry 3 was 3.6 times higher than the number of the Zr complex employed. Since the signals arising from vinylidene and *n*-propyl chain end groups

(Figure 4b) were observed in the polymer obtained by the **2** system, we can conclude β -H elimination from the propagating chain to the Zr species or propylene monomer occurred. The complex **3** activated with dried MAO did not give any polymer, even when polymerization was conducted at 20 °C.

3.3. Polymerization of Propylene Activated with $\text{HNMe}_2\text{PhB}(\text{C}_6\text{F}_5)_4$

Propylene polymerization with **1–3** was investigated using $\text{HNMe}_2\text{PhB}(\text{C}_6\text{F}_5)_4$ as a cocatalyst in the presence of $i\text{Bu}_3\text{Al}$ at 20 °C in toluene under atmospheric pressure. The polymerization results are summarized in Table 4.

(Table 4)

All the complexes showed activity for propylene polymerization under these conditions. **1** showed the highest activity and gave the highest M_n with the broadest M_w/M_n . On the other hand, in the case of **2** and **3**, the M_n value was lower and M_w/M_n value was narrower than that of **1**. Although the N value in entry 5 was almost the same with the number of the Ti complex employed, the consumption rate of propylene, which was measured by a mass flow meter, was stopped within 9 min. The results indicate that this catalyst system was deactivated immediately. The N value in entry 6 was 4.5 times higher than the number of the Zr complex employed, while the N value in entry 7 was about 1/10 of the number of Hf complex employed. These results indicated that chain transfer reaction occurred in the **2** system, while the initiation efficiency was very low in the **3** system.

Figure 5 displays the ^{13}C NMR spectra of the methyl region of the PPs obtained with **1–3**. The **1**- $\text{HNMe}_2\text{PhB}(\text{C}_6\text{F}_5)_4$ system gave slightly syndiotactic-enriched PP ($rr = 43\%$), while the **2** and **3** - $\text{HNMe}_2\text{PhB}(\text{C}_6\text{F}_5)_4$ systems gave highly syndiotactic PPs ($rr \approx 94\%$).

(Figure 5)

The steric pentad fractions of methyl group in main chain determined by ^{13}C NMR spectroscopy. The results are summarized in Table 5.

(Table 5)

The pentad values indicate that the stereospecificity depends on the center metal used. Fujita *et al.* studied propylene polymerization with the group 4 bis[*N*-(3-*tert*-butylsalicylidene)phenylamino] complexes– $\text{Ph}_3\text{CB}(\text{C}_6\text{F}_5)_4\text{-}^i\text{Bu}_3\text{Al}$ systems [13a] and the group 4 bis[*N*-(3-*tert*-butylsalicylidene)-2,3,4,5,6-pentafluoroanilino] complexes–MAO systems. [13b] They found that the mm triads in the former systems increased in the following order: Ti (mm = 22.9%) < Zr (mm = 45.8%) < Hf (mm = 69.0%). On the other hand, in the latter systems, the Ti complex gave a highly syndiotactic (rr = 87%) polymer, but the Zr and Hf complexes gave the non-stereoregular polymers.

The **2**- and **3**- $\text{HNMe}_2\text{PhB}(\text{C}_6\text{F}_5)_4$ systems gave high “rrrr” pentad values of 82% and 86%, respectively, with the stereo defects of “rmmr” arising from the miss selection of prochiral face and “rmrr” arising from the site epimerization. The “rmmr” values are similar in both systems, while the “rmrr” value in the **3**- $\text{HNMe}_2\text{PhB}(\text{C}_6\text{F}_5)_4$ system is lower than that in the **2**- $\text{HNMe}_2\text{PhB}(\text{C}_6\text{F}_5)_4$ system. These stereo defect values indicate that the higher syndiospecificity of the **3**- $\text{HNMe}_2\text{PhB}(\text{C}_6\text{F}_5)_4$ system can be ascribed to the suppression of the site epimerization.

On the other hand, the **1**- $\text{HNMe}_2\text{PhB}(\text{C}_6\text{F}_5)_4$ system gave the lowest “rrrr” value of 20%. The reason why the **1** system gave the lowest stereospecificity PP should be as follows. Chien and co-workers reported the synthesis of isotactic-atactic stereoblock PP with a stereorigid chiral *ansa*-titanocene [30a]. They proposed the mechanism where the polymer chain migrates between two different coordination sites (isospecific and non-stereospecific sites) [30]. The results suggest that the chain migration should more

easily occurred in *ansa*-titanocene than in the corresponding Zr or Hf derivative. The high “rmrr” value (mrrm + rmrr = 26%) supports this assumption. The “rmmr” value in the **1** system is also higher than those of the other systems, which indicates the low enantioselectivity of **1**.

Since the bond angle of N(1)-M(1)-C(4) in **1** (Ti) is larger than those of **2** (Zr) and **3** (Hf) (cf. 3.1.), the steric hindrance around active species is smaller in the case of **1** and hence the enantioselectivity of **1** should be lower than those of **2** and **3**.

Razavi et al. reported that the change of hapticity or the variation of bond order during polymerization should be considered in the syndiotactic specific polymerization of propylene with metallocene catalysts because the haptotropy and ring-slippage can influence the electronic and steric properties of the active site [31]. A plausible change of the coordination mode in the present complexes is shown in Figure 6. If this isomerization occurs more frequently in **1** than in **2** or **3**, the syndiospecificity of **1** should also be decreased due to the C_1 -symmetric structure of the isomers.

(Figure 6)

The signals assignable to vinylidene and *n*-propyl chain end groups (Figure 5b) indicate that β -H elimination also occurred by **2** activated with $\text{HNMe}_2\text{PhB}(\text{C}_6\text{F}_5)_4$. The signals arising from regioirregular units were not observed in all the polymers regardless of the complex used, even when $\text{HNMe}_2\text{PhB}(\text{C}_6\text{F}_5)_4$ was used as a cocatalyst.

4. Conclusion

A series of group 4 dimethyl complexes with a *tert*-butyl(dimethylfluorenylsilyl)amido ligand were synthesized with a facile method and the fluorenyl ligand was found to coordinate to center metal in a η^3 -manner irrespective of center metal employed. The Ti complex activated with dried MAO at 0 °C gave the

syndiotactic-enriched PP with narrow M_w/M_n , whereas the complex gave almost atactic PP with broad M_w/M_n when activated with $\text{HNMe}_2\text{PhB}(\text{C}_6\text{F}_5)_4$ at 20 °C. The Zr complex gave a low-molecular weight syndiotactic PP with vinylidene and *n*-propyl chain end groups irrespective of the cocatalyst employed. The Hf complex polymerized propylene only when activated by $\text{HNMe}_2\text{PhB}(\text{C}_6\text{F}_5)_4$. Although this system showed the lowest catalytic activity, the produced PP had the highest syndiotacticity. It was found that catalytic activity and the stereospecificity were strongly dependent on both the center metal of the *ansa*-fluorenylamidodimethyl complex and the cocatalyst employed.

5. Acknowledgement

We thank Tosoh-Finechem Co., Ltd. for donating MAOs. We thank Dr. Yuushou Nakayama and Mr. Mitsuhiro Okada for useful discussion and EI-MS study (Hiroshima University). We also acknowledge support from the New Energy and Industrial Technology Development Organization (NEDO) under the Ministry of Economy, Trade and Industry (METI), Japan, granting the project on “Nanostructured Polymeric Materials” in the “Material Nanotechnology Program” since 2001.

6. Supplementary material

Crystallographic data have been deposited with the Cambridge Crystallographic Data Centre, CCDC Nos. 274545, 274546 and 274547 for complex **1**, **2** and **3** respectively. Copies of data are obtained free of charge on application to CCDC, 12 Union Road, Cambridge CB2 1EZ, UK (Fax: +44 01223 336033; e-mail: deposit@ccdc.cam.ac.uk).

References

- [1] (a) H.-H. Brintzinger, D. Fischer, R. Mülhaupt, B. Rieger, R. M. Waymouth, *Angew. Chem. Int. Ed. Engl.* 34 (1995) 1143. (b) G. J. P. Britovsek, V. C. Gibson, D. F. Wass, *Angew. Chem. Int. Ed. Engl.* 38 (1999) 428. (c) V. C. Gibson, S. K. Spitzmesser, *Chem. Rev.* 103 (2003) 283.
- [2] (a) P. J. Shapiro, E. Bunel, W. P. Schaefer, J. E. Bercaw, *Organometallics* 123 (1990) 1649. (b) P. J. Shapiro, W. D. Cotter, W. P. Schaefer, J. A. Labinger, J. E. Bercaw, *J. Am. Chem. Soc.* 116 (1994) 4623.
- [3] J. Okuda, *Chem. Ber.* 123 (1990) 1649.
- [4] Eur. 416815 A2 (1991) and U.S. 401345 (1990), Dow Chemical corporation, invs.: J. C. Stevens, F. J. Timmers, D. R. Wilson, G. F. Schmidt, P. N. Nickias, R. K. Rosen, G. W. Knight, S. Y. Lai; *Chem. Abstr.* 115 (1991) 93163m.
- [5] (a) U.S. 5026798 (1991), Exxon Chemical corporation, inv.: J. M. A. Canich; *Chem. Abstr.* 118 (1993) 60284k. (b) U.S. 5055438 (1991), Exxon Chemical corporation, inv.: J. M. A. Canich; *Chem. Abstr.* 118 (1993) 60283. (c) WO 9319103 (1993), Exxon Chemical corporation, inv.: H. W. Turner. G. G. Halatky, J. M. A. Canich; *Chem. Abstr.* 120 (1994) 271442q.
- [6] For example, review articles for olefin polymerization with CpA catalysts; A. L. McKnight, R. M. Waymouth, *Chem. Rev.* 98 (1998) 2587 and references therein.
- [7] (a) F. G. Sernetz, R. Mülhaupt, R. M. Waymouth, *Macromol. Chem. Phys.* 197 (1996) 1071. (b) F. G. Sernetz, R. Mülhaupt, F. Amor, T. Eberle, J. Okuda, *J. Polym. Sci., Part A: Polym. Chem.* 35 (1997) 1571. (c) F. G. Sernetz, R. Mülhaupt, *J. Polym. Sci., Part A: Polym. Chem.* 35 (1997) 2549. (d) G. Xu, *Macromolecules* 31 (1998) 2395. (e) G. Xu, E. Ruckenstein, *ibid.* 31 (1998) 4724. (f) G. Xu, D. Cheng, *ibid.* 34 (2001) 2040.
- [8] (a) J. M. A. Canich; U. S. 5504169, Exxon Chemical corporation, inv. (1996). (b) A.

- L. McKnight, M. A. Masood, R. M. Waymouth, D. A. Straus, *Organometallics* 16 (1997) 2879. (c) L. Resconi, I. Camurati, C. Grandini, M. Rinaldi, N. Mascellani, O. Traverso, *J. Organomet. Chem.* 664 (2002) 5. (d) C. De Rosa, F. Auriemma, O. Ruiz de Ballesteros, L. Resconi, A. Fait, E. Ciaccia, I. Camurati, *J. Am. Chem. Soc.* 125 (2003) 10913 and references therein.
- [9] J. Okuda, F. J. Schattenmann, S. Wokadlo, W. Massa, *Organometallics* 14 (1995) 789.
- [10] H. Hagihara, T. Shiono, T. Ikeda, *Macromolecules* 30 (1997) 4783.
- [11] (a) A. Razavi, V. Bellia, Y. De Brauwer, K. Hortmann, M. Lambrecht, O. Miserque, L. Peters, S. Van Belle, “Metalorganic Catalysts for Synthesis and Polymerization”, W. Kaminsky, Ed., Springer-Verlag, Berlin, 1999, p.236 and references therein. (b) A. Razavi, U. Thewalt, *J. Organomet. Chem.* 621 (2001) 267. (c) V. Busico, R. Cipullo, F. Cutillo, G. Talarico, A. Razavi, *Macromol. Chem. Phys.* 204 (2003) 1269.
- [12] T. Shiomura, T. Asanuma, N. Inoue, *Macromol. Rapid Commun.* 17 (1996) 9.
- [13] (a) J. Saito, M. Onda, S. Matsui, M. Mitani, R. Furuyama, H. Tanaka, T. Fujita, *Macromol. Rapid Commun.* 23 (2002) 1118. (b) H. Makio, Y. Tohi, J. Saito, M. Onda, T. Fujita, *Macromol. Rapid Commun.* 24 (2003) 894 and references therein.
- [14] (a) H. Hagihara, T. Shiono, T. Ikeda, *Macromolecules* 31 (1998) 3184. (b) T. Hasan, A. Ioku, K. Nishii, T. Shiono, T. Ikeda, *Macromolecules* 34 (2001) 3142. (c) K. Nishii, T. Matsumae, E. O. Dare, T. Shiono, T. Ikeda, *Macromol. Chem. Phys.* 205 (2004) 363.
- [15] (a) D. Balboni, G. Prini, M. Rinaldi, L. Resconi, *Am. Chem. Soc. Polym. Prep.* 41 (2000) 456. (b) D. Balboni, I. Camurati, G. Prini, L. Resconi, S. Galli, P. Mercandelli, A. Sironi, *Inorg. Chem.* 40 (2001) 6588. (c) C. Grandini, I.

- Camurati, S. Guidotti, N. Mascellani, L. Resconi, I. E. Nifant'ev, I. A. Kashulin, P. V. Ivchenko, P. Mercandelli, A. Sironi, *Organometallics* 23 (2004) 344 and references therein.
- [16] D. W. Carpenetti, L. Kloopenburg, T. J. Kupec, J. L. Petersen, *Organometallics* 15 (1996) 1572.
- [17] T. Higashi, *Program for absorption correction*; Rigaku Corp.: Tokyo, Japan, 1995.
- [18] *teXsan; Crystal Structure Analysis Package, ver. 1. 11*; Rigaku Corp.: Tokyo, Japan, 2000.
- [19] *International Tables for X-ray Crystallography*; Kynoch Press: Birmingham, 1975; Vol. 4.
- [20] (a) G. M. Sheldrick, *SHELXS-86: Program for crystal structure determination*; University of Göttingen: Göttingen, Germany, 1986. (b) G. M. Sheldrick, *SHELXL-97: Program for crystal structure refinement*; University of Göttingen: Göttingen, Germany, 1997.
- [22] P. T. Beurskens, G. Admiraal, G. Beurskens, W. P. Bosman, S. Garcia-Granda, R. O. Gould, J. M. M. Smits, C. Smykalla, *The DIRDIF program system, Technical Report of the Crystallography Laboratory*; University of Nijmegen: Nijmegen, The Netherland, 1992.
- [22] G. Xu, *Macromolecules* 31 (1998) 2395.
- [23] The crystallographic data of [^tBuNSiMe₂Cp*]TiMe₂ complex: C₁₇H₃₃NSiTi, F.W. = 327.44 g•mol⁻¹, triclinic, space group *Pnma*, *a* = 11.868(2), *b* = 13.398(2), *c* = 12.232(1) Å, *V* = 1945.0(5) Å³, *Z* = 4, *D_c* = 1.118 g•cm⁻³, *R* = 0.0840, *R_w* = 0.211, for 1669 independent reflections with *I* > 2σ(*I*). Selected bond lengths are as follows: Ti(1)–C(3) = Ti(1)–C(5) = 2.350 Å; Ti(1)–C(4) = 2.283 Å; Ti(1)–C(6) = Ti(1)–C(7) = 2.463 Å.

- [24] (a) E. Kirillov, L. Toupet, C. W. Lehmann, A. Razavi, S. Kahlal, J.-Y. Saillard, J.-F. Carpentier, *Organometallics* 22 (2003) 4038. (b) E. Kirillov, L. Toupet, C. W. Lehmann, A. Razavi, J.-F. Carpentier, *Organometallics* 22 (2003) 4467 and references therein.
- [25] M. H. Lee, J.-W. Hwang, Y. Kim, J. Kim, Y. Han, Y. Do, *Organometallics* 18 (1999) 5124.
- [26] W. J. Evans, T. S. Gammersheimer, T. J. Boyle, J. W. Ziller, *Organometallics* 13 (1994) 1281.
- [27] L. J. Irwin, S. A. Miller, *J. Am. Chem. Soc.* 127 (2005) 9972.
- [28] H. G. Alt, K. Föttinger, W. Milius, *J. Organomet. Chem.* 572 (1999) 21.
- [29] (a) S. Gentil, M. Dietz, N. Pirio, P. Meunier, J. C. Gallucci, F. Gallou, L. A. Paquette, *Organometallics* 21 (2002) 5162. (b) S. Deisenhofer, T. Feifel, J. Kukral, M. Klinga, M. Leskelä, B. Rieger, *Organometallics* 22 (2003) 3495 and references therein.
- [30] (a) D. T. Mallin, M. D. Rausch, Y.-G. Lin, S. Dong, J. C. W. Chien, *J. Am. Chem. Soc.* 112 (1990) 2030. (b) G. W. Coates, *Chem. Rev.* 100 (2000) 1223 and references therein.
- [31] A. Razavi, D. Baekelmans, V. Debrwer, K. Hortmann, M. Lambrecht, O. Miserque, M. Slawinski, L. Peters, S. Van Belle, in: T. Sano, T. Uozumi, H. Nakatani, M. Terano (Eds), *Progress and Development of Catalytic Olefin Polymerization, Technology and Education Publishers, Tokyo, 2000, p. 176 and references therein.*

Figure captions

Scheme 1. Synthetic procedure for group 4 *ansa*-fluorenylamidodimethyl complexes

Chart 1. Bonding modes of complexes that contains the fluorenyl ligand

Figure 1. ORTEP drawing of **1**. Hydrogen atoms are omitted for clarity. The thermal ellipsoids are drawn at the 30% probability level.

Figure 2. ORTEP drawing of **2**. Hydrogen atoms are omitted for clarity. The thermal ellipsoids are drawn at the 30% probability level.

Figure 3. ORTEP drawing of **3**. Hydrogen atoms are omitted for clarity. The thermal ellipsoids are drawn at the 30% probability level.

Figure 4. 125 MHz ^{13}C NMR spectra of methyl region of polypropylenes obtained with **1** and **2**–dried MAO at 0 °C: (a) **1** in entry 1; (b) **2** in entry 3.

Figure 5. 125 MHz ^{13}C NMR spectra of methyl region of polypropylenes obtained with **1**, **2** and **3**–HNMe₂PhB(C₆F₅)₄ at 0 °C: (a) **1** in entry 5; (b) **2** in entry 6; (c) **3** in entry 7.

Figure 6. A plausible scheme of ring-slippage in group 4 *ansa*-fluorenylamidodimethyl complexes.

Table 1. Crystallographic data and parameters for 1, 2 and 3

	1 (Ti)	2 (Zr)	3 (Hf)
formula	C ₂₁ H ₂₉ NSiTi	C ₂₁ H ₂₉ NSiZr	C ₂₁ H ₂₉ NSiHf
formula weight	371.45	414.77	502.04
crystal system	monoclinic	orthorhombic	orthorhombic
space group	<i>C2/c</i>	<i>Pnma</i>	<i>Pnma</i>
<i>a</i> (Å)	24.707(4)	8.3517(3)	8.3597(3)
<i>b</i> (Å)	12.215(2)	14.4219(5)	14.436(1)
<i>c</i> (Å)	14.293(7)	16.8132(6)	16.869(1)
β (deg)	113.176(4)		
<i>V</i> (Å ³)	3965(1)	2025(1)	2035(1)
<i>Z</i>	8	4	4
<i>F</i> (000)	1584	864	992
<i>D</i> calcd (g·cm ⁻³)	1.244	1.360	1.638
μ (mm ⁻¹)	0.494	0.604	5.176
max. 2θ (deg)	55	55	55
no. of reflections observed	4280	15808	15843
no. of parameters refined	333	177	121
<i>R</i> 1 ^a	0.0563	0.0361	0.0430
w <i>R</i> 2 ^b	0.1595	0.1010	0.1249
no. of obsd reflns ($I > 2\sigma(I)$)	3860	2096	2222

^a $R1 = [\sum||F_o| - |F_c||]/\sum|F_o|$. ^b $wR2 = [\sum[w(F_o^2 - F_c^2)^2]/\sum[w(F_o^2)^2]]^{1/2}$.

Table 2. Selected bond lengths (Å) and angles (deg) for 1, 2 and 3

	1 (Ti)	2 (Zr)	3 (Hf)
Lengths			
M(1)–C(1)	2.105(3)	2.244(3)	2.223(6)
M(1)–C(2)	2.106(3)	2.244(3)	2.223(6)
M(1)–C(3)	2.415(3)	2.529(2)	2.515(3)
M(1)–C(4)	2.253(3)	2.404(3)	2.401(5)
M(1)–C(5)	2.418(3)	2.529(2)	2.515(3)
M(1)–C(6)	2.572(3)	2.672(2)	2.664(3)
M(1)–C(7)	2.573(3)	2.672(2)	2.664(3)
M(1)–N(1)	1.923(3)	2.063(2)	2.046(4)
M(1)–Si(1)	2.836(1)	2.989(7)	2.967(1)
Angles			
N(1)–M(1)–C(4)	78.3(10)	72.9(9)	73.9(2)
M(1)–N(1)–Si(1)	101.0(1)	103.6(1)	103.0(2)
N(1)–Si(1)–C(4)	94.2(1)	95.7(1)	96.1(2)

Table 3. Results of propylene polymerization with [*t*-BuNSiMe₂Flu]MMe₂-dried MAO catalysts^a

entry	cat.	temp. (°C)	A ^b	M _n ^c (× 10 ³)	M _w /M _n ^c	N ^d (μmol)	rr ^e (%)	T _m ^f (°C)
1	1 (Ti) ^g	0	257	157	1.22	16	63	- ^h
2	2 (Zr)	0	- ⁱ	-	-	-	-	-
3	2 (Zr)	20	11	1.53	1.99	72	97	124
4	3 (Hf)	0, 20	- ⁱ	-	-	-	-	-

^a Polymerization conditions: toluene = 30 mL, M (Ti, Zr, Hf) = 20 μmol, dried MAO = 8.0 mmol, propylene = 1 atm, 30 min. ^b Activity in kg-PP•mol-Ti⁻¹•h⁻¹. ^c Determined by GPC using universal calibration. ^d Number of polymer chains calculated from yield and M_n. ^e Determined by ¹³C NMR. ^f Determined by DSC. ^g See ref. 14b in detail. ^h Not detected. ⁱ Not polymerized.

Table 4. Results of propylene polymerization with $[t\text{-BuNSiMe}_2\text{Flu}]MMe_2\text{-HMe}_2\text{NPhB}(\text{C}_6\text{F}_5)_4$ catalyst^a

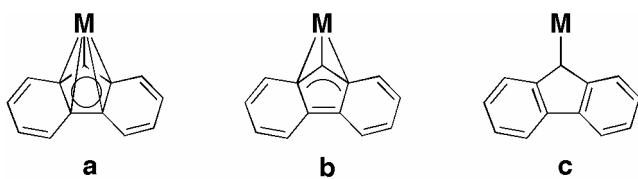
entry	cat.	time (min)	A^b	M_n^c ($\times 10^3$)	M_w/M_n^c	N^d (μmol)	rr ^e (%)	T_m^f ($^\circ\text{C}$)
5	1 (Ti)	9	143.3	19.8	3.22	43	43	- ^g
6	2 (Zr)	20	22.7	1.68	1.26	180	92	115
7	3 (Hf)	30	0.56	3.06	1.48	3.7	95	129

^a Polymerization conditions: toluene = 30 mL, M (Ti, Zr, Hf) = B = 40 μmol , $i\text{Bu}_3\text{Al}$ = 800 μmol , propylene = 1 atm, 20 $^\circ\text{C}$. ^b Activity in $\text{kg-PP}\cdot\text{mol-Ti}^{-1}\cdot\text{h}^{-1}$. ^c Determined by GPC using universal calibration. ^d Number of polymer chains calculated from yield and M_n . ^e Determined by ^{13}C NMR. ^f Determined by DSC. ^g Not detected.

Table 5. ^{13}C NMR analysis of polypropylenes obtained with 1, 2 and 3

pentad distributions	1 (Ti) (entry 5)	2 (Zr) (entry 6)	3 (Hf) (entry 7)
mmmm	0.01	0.00	0.00
mmmr	0.04	0.00	0.00
rmmr	0.05	0.01	0.01
mmrr	0.10	0.03	0.03
mrmr + rmrr	0.26	0.04	0.01
rmm	0.11	0.00	0.00
rrrr	0.20	0.82	0.86
mrrr	0.19	0.09	0.09
mrrm	0.04	0.01	0.00

Scheme 1.



M = transition metal

Chart 1.

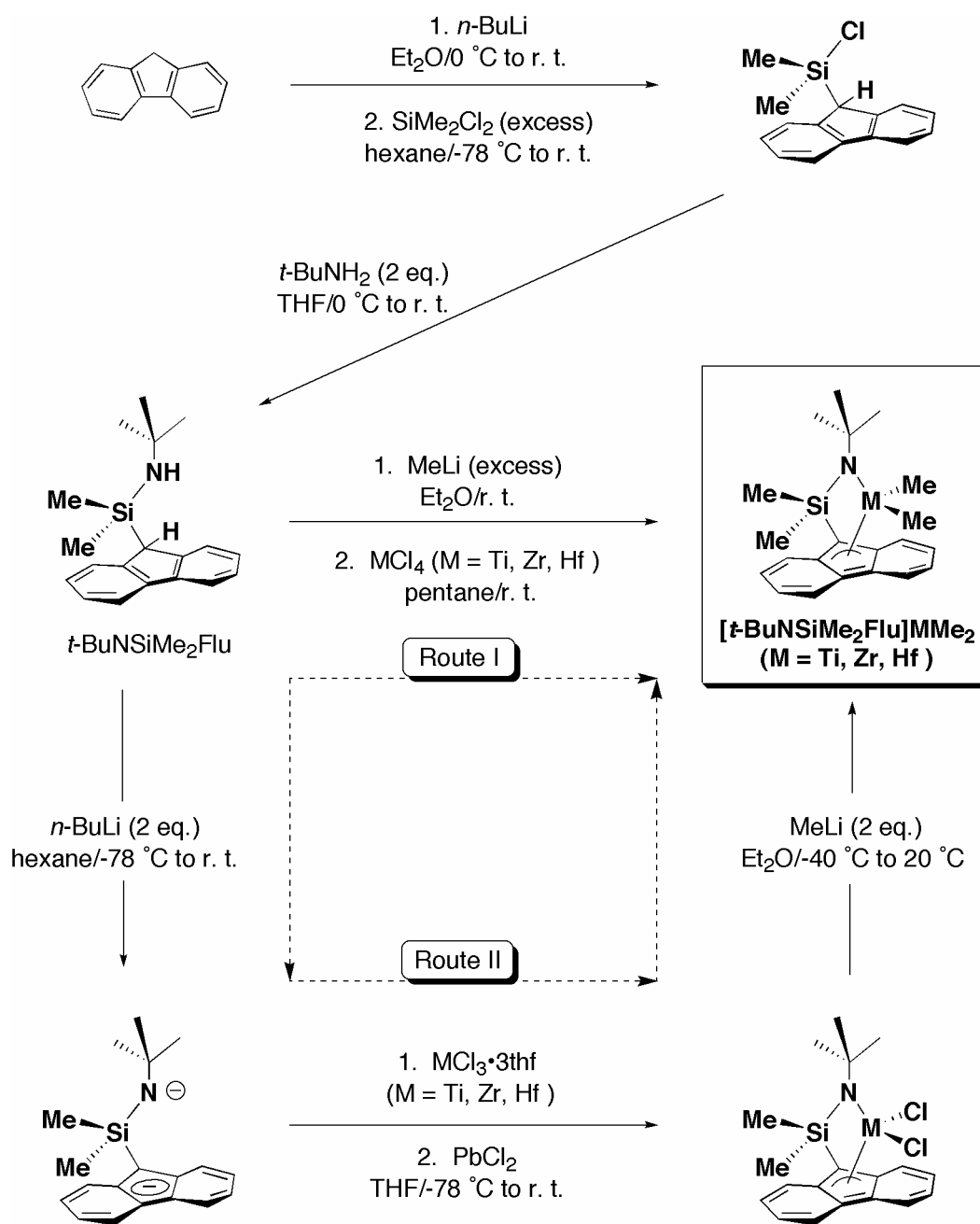


Figure 1.

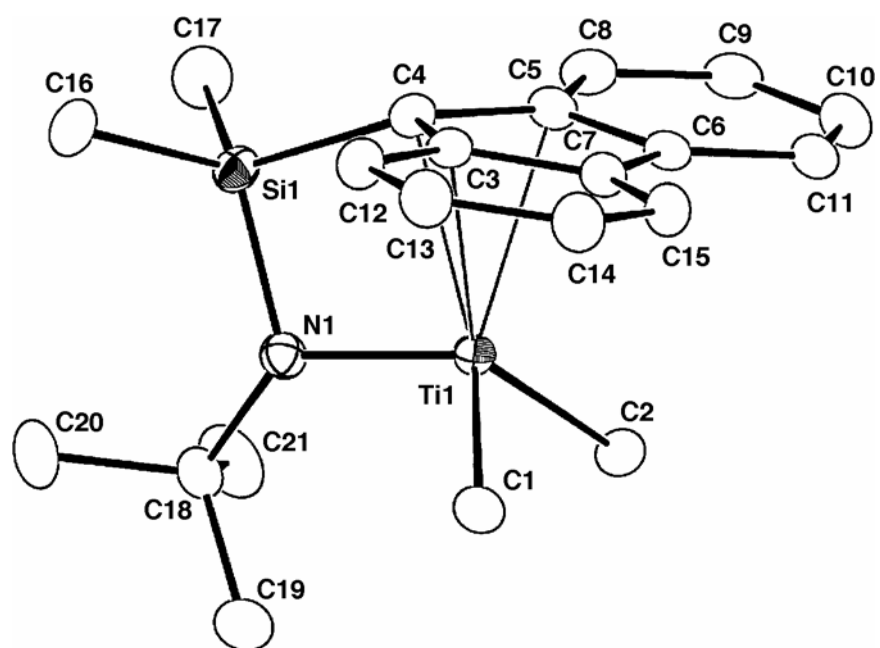


Figure 2.

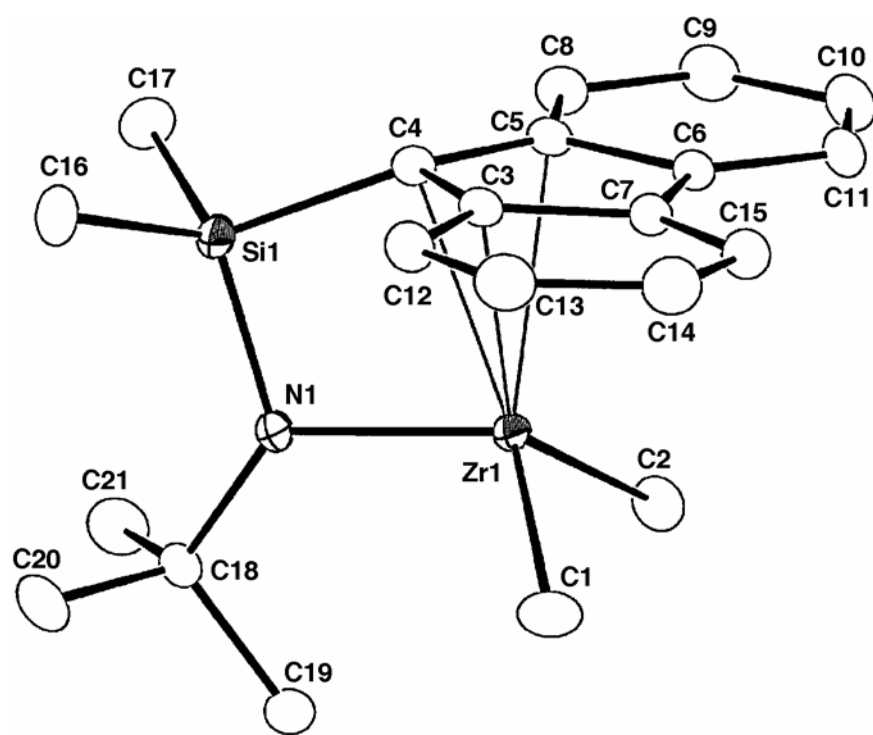


Figure 3.

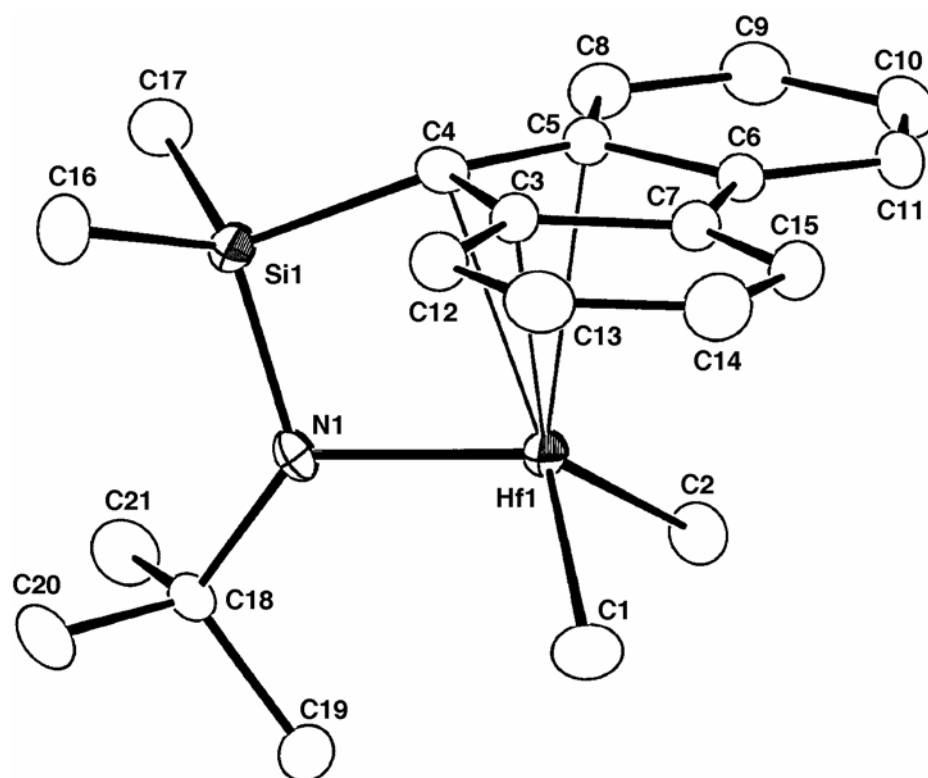


Figure 4.

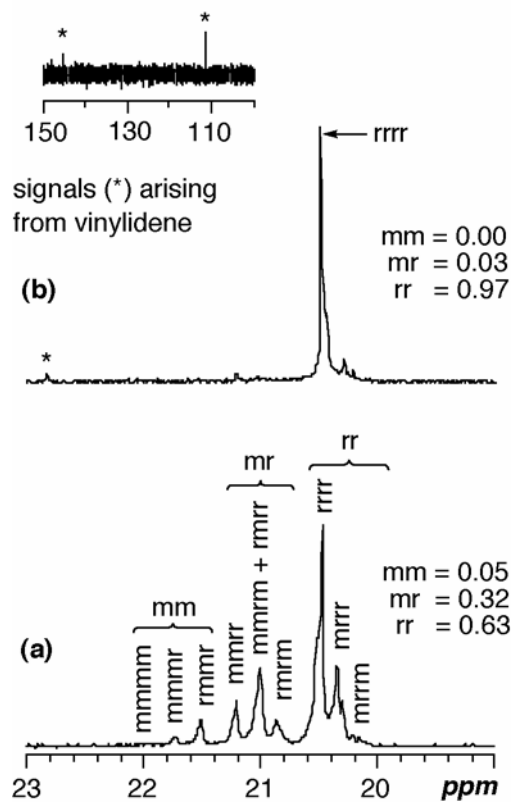


Figure 5.

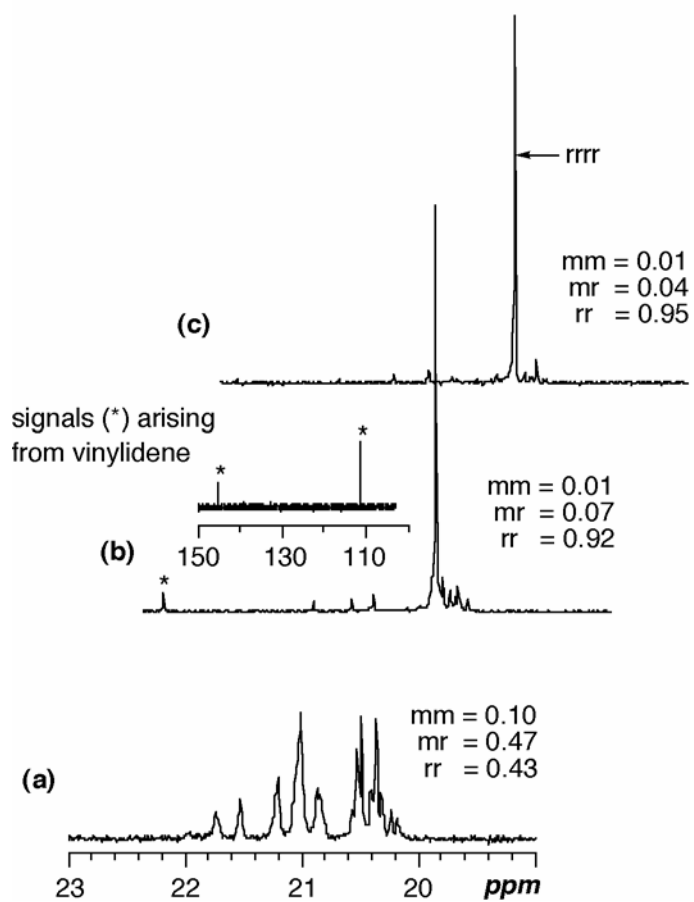


Figure 6.

